PCCP

Accepted Manuscript

ROYAL SOCIETY OF CHEMISTRY

www.rsc.org/pccp

Cite this: DOI: 10.1039/c0xx00000x

www.rsc.org/xxxxxx

ARTICLE TYPE

ZnO–Ag hybrids for ultrasensitive detection of trinitrotoluene by surface-enhanced Raman spectroscopy

Xuan He,*[a] Hui Wang,[a] Zhongbo Li,*[b] Dong Chen [a] and Qi Zhang*[a]

Received (in XXX, XXX) Xth XXXXXXXXX 20XX, Accepted Xth XXXXXXXXX 20XX

DOI: 10.1039/b000000x

An efficient and green approach was used to fabricate novel and low-cost surface-enhanced Raman scattering (SERS) spectroscopy sensors based on 4-aminothiophenol (4-ATP) functionalized ZnO–Ag hybrid nanoflowers for the detection of explosives. Such SERS sensors exhibited high sensitivity to rhodamine 6G (R6G) at a low concentration of 10^{-12} M and an enhancement factor of over 4.12×10^6 was achieved. Moreover, the Raman-inactive trinitrotoluene (TNT) initiated the high Raman scattering of non-resonated 4-ATP through the formation of a π-donor–π-acceptor interaction between the π-acceptor, TNT, and the π-donor, 4-ATP-Ag-ZnO complex, on the flower-like hybrids. Because this π-donor–π-acceptor interaction could effectively induce the "hot spots" for SERS, TNT concentrations as low as 5×10^{-9} M could be detected. Furthermore, other derivatives of TNT were also explored, and this sensor exhibited better selectivity for TNT than other similarly structured explosives. The low-cost hybrid SERS substrates presented good sensitivity and reproducibility for the analytes employed, demonstrating promising application in forensic science and homeland security.

Introduction

Detection of nitrated explosives, especially trinitrotoluene (TNT), one of the most notorious, highly explosive nitroaromatic compounds with significant deleterious effects on the environment and human health, is a matter of tremendous societal concern.[1] Moreover, TNT has also been used in military and terrorist activities in recent years, which is posing the threat to homeland security. Therefore, developing sensitive and real-time analytical detection methods for explosives have attracted considerable research attention due to the ever-increasing needs for a secure and peaceful environment.[2]

In recent years, a variety of methods for analyzing TNT have been explored, such as fluorescent sensors,[3] organic polymers,[4] or fluorescent silicon nanoparticles (NPs),[5] which are based on the quenching or enhancing of fluorescence intensity. In terms of biosensors, the signals change when the antibody-based optical or voltammetric sensor react with TNT.[6] Colorimetric sensors rely on changes of the absorbance which are caused by the aggregation of metal nanoparticles in the presence of nitrated explosives.[7] Among these sensors, spectroscopic sensors based on surface-enhanced Raman spectroscopy (SERS) have attracted much attention due to the perspectives of both fundamental understanding and practical applications.[8]

Surface-enhanced Raman scattering spectroscopy as one of the most useful ultra-sensitive real-time analytical techniques has led to major breakthroughs in a number of areas.[9] However, the strength of SERS signals is critical for applications of the technology, which is strongly dependent on the morphology of SERS substrates . Thus, it is highly desirable to construct SERS substrates with sufficient highly active SERS hot spots, which could ensure the high SERS detection signals.[10] In theory, the enhancement effects have been widely accepted as "electromagnetic mechanism (EM)" and "chemical mechanism (CM)". Composites or heterostructures of semiconductors and noble metals, such as ZnO–Ag, exhibit much higher SERS effect because of the contributions from both the electromagnetic enhancement (excited by the localized surface plasmon resonance of noble metals) and the semiconductor supporting chemical enhancement (caused by the charge transfer between the noble metal and the adjacent semiconductor).[11] From this viewpoint, SERS effect of semiconductors and noble metals hybrid nanostructures could provide important insight into coexistence of the EM and CM effects among the semiconductors, noble metals, and adsorbed analytes.[12] In addition, it has been demonstrated that hybrid SERS substrates (graphene/Ag, Fe_3O_4 /Au) have very good prospects in terms of TNT detection and modification of the 4-aminothiophenol (4-ATP) molecule as a probe could increase the adsorption efficiency, thereby reduce the detection limit.[13a, b] Thus, the as-prepared semiconductors and noble metals hybrids can be functionalized with 4-ATP to form composited SERS sensors, which appear to be as an efficient approach for the detection of TNT and other explosives.[13]

In this work, we successfully prepared ZnO–Ag hybrid nanoflowers by combining the hydrothermal method with electron-beam evaporation deposition. First, the as-prepared ZnO–Ag hybrid was functionalized with 4-ATP which acted as a probe and could interact with TNT and provide exceptionally strong enhancement in Raman scattering as the CM effect. Then, the TNT-induced enhancement of the 4-ATP Raman signal was

realized, which could be used to detect TNT with a low concentration of 5 × 10^{-9} M. Furthermore, their derivatives of TNT were also explored, and the sensor exhibited better selectivity for TNT than other similarly structured explosives. In addition, tentative assignment of molecule Raman peaks was done with the assistance of a quantum mechanics (QM) calculation, and the structures of Raman peaks have been identified. Finally, the mechanism of the 4-ATP probe was also studied. As such, the 4-ATP-functionalized ZnO–Ag hybrid could serve as an excellent SERS platform for TNT detection with high sensitivity, selectivity and reproducibility.

Experimental section

Materials

Chemicals and Reagents. $Zn(NO_3)_2 \cdot 6H_2O$ (Advanced Pure 99.998%), rhodamine 6G(R6G Advanced Pure 95%), hexamethylenetetramine (HMT Advanced Pure 95%), 4-aminothiophenol (4-ATP, $4\text{-}NH_2C_6H_4SH$) were all purchased from Aladdin Chemistry Co. Ltd., China. Ethanol (AR) was all purchased from Longke Co., China. Ultrapure water from Milli-Q source was used throughout the experiments. All reagents were used as received without further purification. 2, 4, 6-Trinitroboluene (TNT, $C_7H_5N_3O_6$), picric acid (PA, $C_6H_3N_3O_7$), 2-nitrotoluene (2-NT, $C_7H_7NO_2$) and 2, 4-dinitrotoluene (DNT, $C_7H_6N_2O_4$) was pured from ICM. N-type Si (100) was cleaned sequentially with acetone, ethanol and deionized water for 15min respectively, then dried with nitrogen flow.

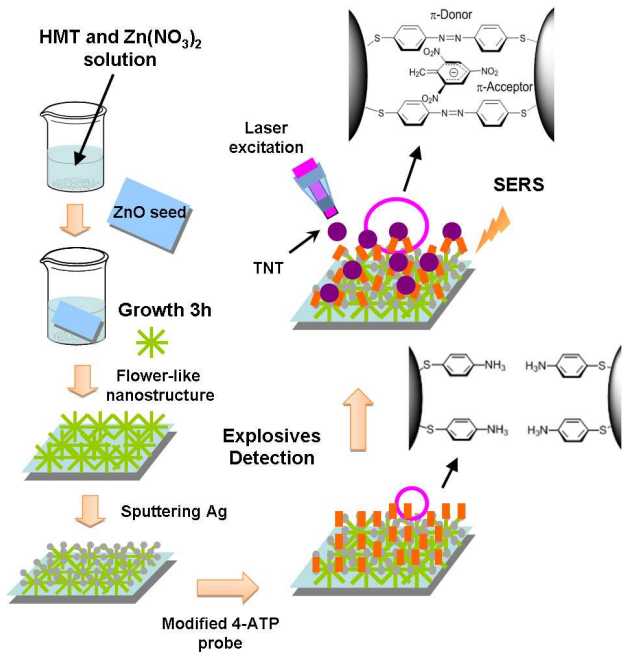

Scheme 1. Schematic image of the fabrication process for the ZnO-Ag hybrids and the detection section of explosives.

Preparation of ZnO flower-like nanostructures

Briefly，the 0.375M $ZnAc_2 \cdot 2H_2O$ was dissolved in the pre-mixed solution of ethanolamine and 1, 2-dimethoxyethane. The proportion of ethanolamine and 1, 2-dimethoxyethane was 1:1. After stirring for 30min, a clear solution was obtained. Then the dip-coating method was used for obtain zinc oxide gel film. The clean silicon substrate was dipped in zinc oxide gel film within 1 min, and then pulled with the speed 0.8 mm/s by gel instrument, dried at 80°C. These processes were repeated three times. And then the substrate coated with a thin film was heat-treated for 2 hours at 550°C to obtain a seed crystal film. After seeding, hydrothermal growth of ZnO nanoflowers (NFs) was performed in a thermal container. 0.05 M solution of $Zn(NO_3)_2 \cdot 6H_2O$ and 0.05 M solution of HMT in distilled water were prepared and equal volume aliquots of each solution were mixed together. All the chemicals were analytical grade and used without further purification. Before introducing the substrate into the growth solution, the precursor solution was maintained in a laboratory hydrothermal chamber at 93℃ for 1 h to stabilize the growth temperature. The Si wafers with ZnO seed were inserted into the precursor solution at an acute angle and maintained at 93℃ for 3h. The as-prepared samples were rinsed in deionized water, and then dried in oven at 70℃.

Preparation of ZnO-Ag NF hybrids

The ZnO nanostructures were coated with Ag nanoparticles by sputtering (EMITECH K550X sputter coater) at room temperature. Before deposition, the vacuum chamber of pressure was decreased down to 1×10^{-1} mbar. And different deposition times from 4 to 26 min with a current of 30 mA were used for optimized conditions.

SERS spectra Measurement

ZnO-Ag NF hybrids were used as SERS substrates for SERS measurement. 4-ATP solution was diluted to 1×10^{-8} M with ethanol. In order to ensure molecule adsorption equilibrium, the SERS substrates were immersed into the 4-ATP solution for 3 h. In this experiment, to verify the stability and reproducibility of these SERS active substrates, more than five SERS-active substrates of each ZnO-Ag hybrids were prepared, and fifteen different points on each substrate were selected to detect the 4-ATP probe. Next, 10 μL of TNT with different concentrations in ethanol was dropped onto the SERS substrate which was modified with 4-ATP probe, and the solvent was allowed to evaporate under ambient conditions. The substrates were then taken out and rinsed with deionized water. Raman measurements were conducted with a FT-Raman spectrometer (DXRsmart Raman) equipped. The excitation source was 532 nm excitation. In order to avoid the catalytic and photochemical decomposition caused by laser exposure, the laser power at the sample position was 8.0 mW, the laser beam was focused on the sample in a size of about 2 μm, and the typical accumulation time used for the study was 5 s. At least 5 points of each sample were collected and each point was tested twice to ensure the reproducibility.

Results and discussion

Structure characterization of ZnO and ZnO-Ag NF hybrids

The as-prepared ZnO NFs on the substrate were characterized by field-emission scanning electron microscopy (FE-SEM). As shown in Figure 1, ZnO NFs with average diameters of about 3μm consisting of nanorods with diameters of about 200 nm were

obtained (Figure 1a, b). SEM images showed that the flowers were uniform in shape and size, with the centres as common growth points for all of the constituent nanorods. In the powder X-ray diffraction (XRD) patterns, the sharp diffraction peaks indicated the excellent crystalline nature of all the samples, and all peaks could be indexed to the hexagonal structure of ZnO (Joint Committee on Powder Diffraction Standards, JCPDS card No. 36-1451, see Figure S1). Moreover, the transmission electron microscopy (TEM) images further confirmed that the hybrid flowerlike structures were constructed from orderly radial nanorod arrays with the rod oriented lengthwise from the centre to the surface of the flower (Figure 1c). High-resolution TEM (HR-TEM) images (Figure 1d) displayed clear lattice fringes and revealed the single-crystalline nature of an individual ZnO-Ag. Among them, the measured lattice spacing was about 0.52 nm, which corresponded to the (0001) lattice plane of wurtzite ZnO.[14] And the lattice spacing of 0.24 nm matched with the fcc Ag (111) plane, which well agreed with the XRD results as shown in supporting information Figure S1.

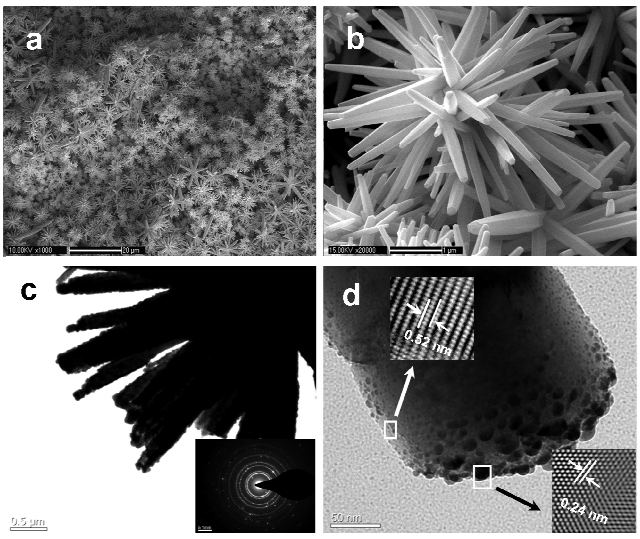

Figure 1. (a) FE-SEM image of ZnO nanostuctures; (b) the enlarged FE-SEM image of ZnO nanostuctures; (c) TEM image of as-presented ZnO-Ag samples; (d) HRTEM images of as-presented ZnO-Ag samples of (c).

Then, ion sputtering was performed to assemble Ag-NPs onto the ZnO NFs with different durations (4min, 16min, and 26min, Figure S2). It should be noted that Ag-NPs and Ag spheres with different dimensions could be assembled simultaneously by simple physical ion-sputtering without any reagents. And also it was obviously observed that prolonging the ion-sputtering duration could increase the size of the Ag-NPs (Figure S2a-f). The surface diffuse reflection UV-vis absorption experiment of ZnO-Ag hybrids revealed the broad plasmon absorption band peaking at 386 nm, which were mainly attributed to the surface plasmon absorption band of Ag nanoparticles (Figure S3). Consequently, together with the facile and efficient controllable synthesis approach of ZnO, decorating with Ag-NPs with non-reagents method, our work presented a clean and green way that circumvents potential Raman spectral interference caused by the chemical modification agents.

SERS characterization of ZnO-Ag hybrids

Next, the SERS activity of as-prepared ZnO-Ag hybrids was investigated by using 10^{-8} M rhodamine 6G (R6G) as the target analyte. As shown in the Figure S4, the SERS activity of the as-prepared substrate improved with increasing Ag-sputtering duration from 4 min to 35min, and the similar Raman intensity was obtained with sputtering durations of 26 min and 35min. According to these SERS detection results, 26 min was chosen the Ag-sputtering duration to fabricate hybrids substrates while maintaining other measurement conditions the same.

To further reveal the good SERS enhancement effect of the hybrid substrates, the substrates were immersed in R6G solutions with concentrations from 10^{-8} to 10^{-12} M. And the resulting Raman spectra were shown in Figure 2a. Four important bands at 611, 771, and 1360 cm^{-1} were identified clearly, even at a concentration as low as 10^{-12} M. In order to demonstrate these semiconductor-noble metal hybrids could produce a much higher SERS effect than a single noble metal, ZnO NFs and clean Si-slide were used to prepare ZnO-Ag hybrids and single Ag-NPs substrate with the same Ag-sputtering durations (26 min) respectively. The compared Raman experimental data was shown in Figure S5, the Raman intensity at 611 cm^{-1} of R6G under ZnO-Ag hybrids substrate was nearly 10 times higher than single Ag NPs substrate, demonstrating that the SERS activity of as prepared ZnO-Ag hybrids was higher than that of single Ag-NPs substrate.

The SERS enhancement factors (EF) for R6G on the ZnO-Ag NFs could be calculated according to the equation $EF=(I_{SERS}/I_{bulk})(N_{bulk}/N_{surface})$, where I_{SERS} and I_{bulk} were the peak intensities of 10^{-10} M R6G on the ZnO-Ag NFs substrate and 1×10^{-3} M R6G on a silicon substrate at 611cm^{-1}, respectively (See Figure S6-S7). N_{SERS} and N_{bulk} were the number of R6G molecules excited by the laser beam on the ZnO-Ag NFs substrate and Si substrate, respectively. The calculated EF of the ZnO-Ag NFs substrate was about 4.12×10^{6}.

Additionally, the reproducibility of SERS signal was also checked by examining 15 random spots across the whole substrate using 10^{-8} M R6G under the same the laser power and the integration time. The results showed good reproducibility in intensity (Figure 2b). Moreover, the relative standard deviation (RSD) of major R6G characteristic SERS peaks were calculated to evaluate the reproducibility of SERS signals. As shown in Figure S8, it was revealing almost the same intensity for each characteristic band of R6G. The maximal RSD value of signal intensities of major SERS peaks was observed to be below 0.25, indicating that ZnO-Ag NFs hybrid SERS substrates had a good reproducibility across the entire area.[15] The experimental results indicated that the ZnO-Ag NFs had high sensitivity, good reproducibility and reliability as the substrate for Raman applications. It was believed that this ZnO-Ag NFs hybrid substrate could be regarded as the highly sensitive SERS substrate. ZnO-Ag hybrids gave rise to this superior SERS activity most likely because of those reasons: 1) these nanorods with the lightning-rod-type morphology could produce more "hot spots" for stronger local electric field enhancement due to different sized Ag-NPs on the side surfaces and top ends of

nanorods which could construct SERS surface and promote the excellent SERS activity (an electromagnetic enhancement effect). 2) Based on the chemical SERS enhancement effect, these semiconductor-noble metal hybrids could produce a much higher SERS effect than a single noble metal due to the contributions from both the electromagnetic enhancement (excited by the localized surface plasmon resonance of noble metals) and the semiconductor supporting chemical enhancement.

SERS study and limit of explosives detection

The observed large enhancement suggested that the ZnO–Ag NF hybrid could indeed serve as a robust solid substrate for carrying out molecular sensing with high sensitivity. Then, the substrates were immersed in 4-ATP solutions with concentrations that varied from 10^{-7} to 10^{-11} M; the Raman spectra of the substrates were shown in Figure S9-S10. Four important bands at 1065, 1135, 1382, 1430, and 1569 cm^{-1} were clearly identified even at a concentration as low as 10^{-11} M.

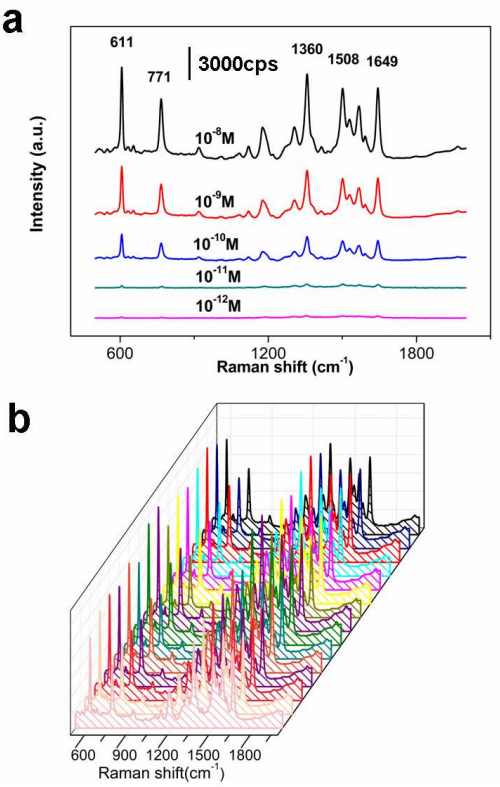

Figure 2. a) The SERS spectra of R6G collected on the ZnO-Ag hybrid substrates with Ag-sputtering for 26 min after being exposed to different concentrations of R6G in alcohol solution; the data acquisition time was 5s. b) A series of SERS spectra of R6G molecules collected on randomly selected 15 places of the ZnO-Ag hybrid substrates.

Then, the substrates were modified with 4-ATP through the formation of Ag–S bonds by immersing them in very dilute 4-ATP ethanol (1×10^{-8} M). And these 4-ATP functionalized ZnO–Ag hybrids were used for the detection of explosives. The Raman responses from pure TNT and pure 4-ATP on a blank substrate (Si wafer), and TNT (dissolved in ethanol) dispersed on unmodified and 4-ATP-modified ZnO–Ag hybrid substrates were shown in Figure S11. Tentative assignment of peaks was completed with the assistance of a quantum mechanics (QM) calculation, and the structure was optimized at the B3LYP-6-311G ++ (d, p) level of theory by Gaussian 03 (see Figure S12 and S13).[17a]

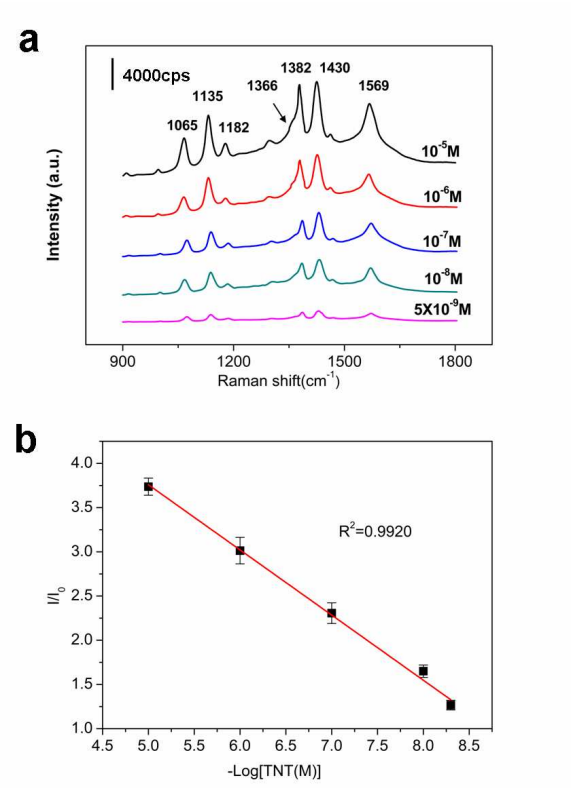

Figure 3 a) Raman responses of 4-ATP-functionalized ZnO-Ag hybrids with the presence of TNT at different concentrations: 10^{-5} to 5×10^{-9} M; b) The corresponding calibration curve for SERS intensity versus –log [TNT], in which the SERS intensities were recorded at 1430cm^{-1}.

The neat wavelength (Figure S13) had minor shifts in the frequencies of some bands, particularly for modes at 1616 and 1365 cm^{-1} and a weaker feature at 1167 cm^{-1}. And these wavelength could all be assigned to TNT as following, the C=C aromatic stretching vibration (1616 cm^{-1}), NO_2 asymmetric stretching vibration (1527 cm^{-1}), NO_2 symmetric stretching vibration (1365 cm^{-1}), and C_6H_2–C vibration (1206 cm^{-1}). Previously reported results showed that the normal Raman spectrum of 4-ATP was mainly characterized by two strong bands.[17] In Figure 3a, the two main peaks at 1065 and 1569 cm^{-1} corresponded to the totally symmetric C–S stretching mode and C–C stretching modes. By comparing the line (1), (2) and (3) in Figure S14, new strong Raman peaks were also observed at 1382 and 1430 cm^{-1}. The previously theoretical and experimental studies assigned these peaks to the N=N vibration of the p, p'-dimercaptoazobenzene (DMAB) vibrational modes.[13a, c] With the addition of TNT, the two peaks were much stronger than those of the a_1 modes of 4-ATP (line (3) peaks at 1065 cm^{-1}, and 1569 cm^{-1}). As shown in Figure 3a, the peak of TNT around 1366 cm^{-1} became the left shoulder of the strong 4-ATP Raman peak at

1382 cm^{-1}. As the concentration of TNT was increased from 5 × 10^{-9} to 1 × 10^{-5} M, the Raman intensity of 4-ATP increased. Also the Raman signals of DMAB were significantly enhanced. The peak intensity at 1430 cm^{-1} was about 3.6 times stronger than that obtained without TNT. These results demonstrated that 4-ATP were paired together to form the corresponding DMAB when 4-ATP was modified on the Ag-NPs. And the Raman signals of TNT might be detected by chemical enhancement technology upon the formation of the DMAB–TNT complex (Scheme 1). In general, the Raman peaks of the TNT molecules were often so weak that these peaks were usually obscured by the relatively strong Raman signals of 4-ATP. As a result, the weak Raman signals of TNT could be observed only at a relatively high concentration. Figure 3b illustrated the linear relationship between the Raman intensity (at 1430 cm^{-1}) and the logarithm of TNT concentration in the range of 5 × 10^{-9} to 1 × 10^{-5} M. From the linear regression equation y = 7.442 - 0.738x, the square of the correlation coefficient was calculated to be 0.9920. The measurements strongly demonstrated that 4-ATP-modified ZnO–Ag NF hybrids could be used as a promising SERS platform for sensitive TNT detection.

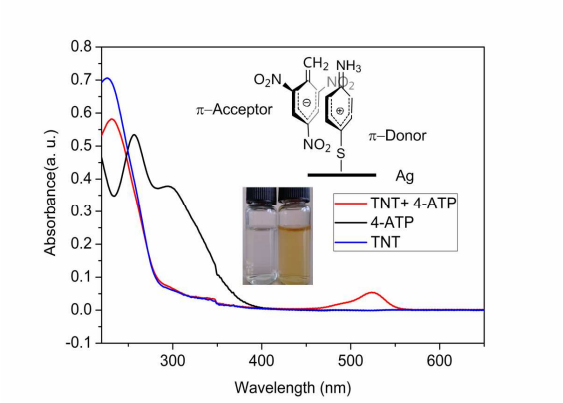

Figure 4. UV-vis absorption spectra of TNT, 4-ATP, TNT and 4-ATP complex. The inset images showed the colours with the addition of 0 and 150μ L of 0.01M 4-ATP into 4mL of 0.1mM TNT solution, respectively. And the inset structures showed the interaction between π-acceptor and π-donor. The UV-vis spectra in solution were obtained using ethanol as the solvent at room temperature with a path-length of 1cm.

The interaction mechanism for TNT detection

Using the 4-ATP-modified ZnO–Ag NF hybrids, we proposed here a mechanism for enhancement of the 4-ATP Raman intensity resulting from TNT-induced resonance. As shown in the inset of Scheme 1, the 4-ATP molecules were strongly adsorbed on the surface of Ag NPs through the formation of the Ag–S chemical bond between the thiol group and Ag NPs. After 4-ATP reached adsorption equilibrium, the TNT assembly was formed just by simply mixing the TNT ethanol solutions with the 4-ATP-modified ZnO–Ag hybrids.[18] Moreover, the TNT molecules were immediately captured by the 4-ATP probe through the formation of the 4-ATP–TNT complex. It had been confirmed that the TNT molecule was deprotonated at the methyl group by the electron-rich amine, leading to the formation of the charge-transfer Meisenheimer complex.[19] The negative charge on the TNT anion was distributed throughout the aromatic ring through the resonance stabilization by three electron-withdrawing nitro-

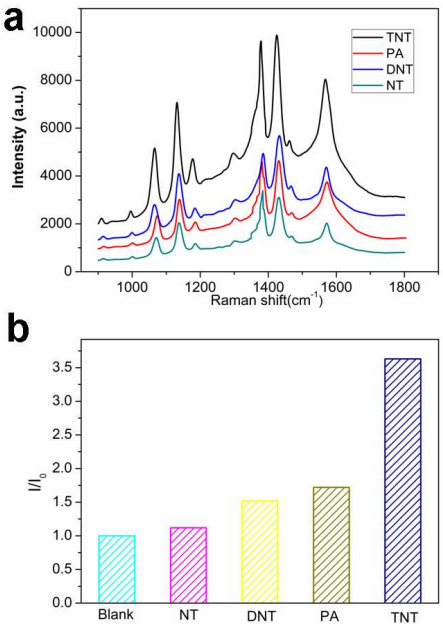

Figure 5 a) Raman spectra of ZnO-Ag with the presence of various TNT structure-like molecules: 2-nitrotoluene (2-NT), 2, 4-dinitrotoluene (DNT), and 2, 4, 6-Trinitroboluene (TNT), with the same concentration of 10^{-7} M in ethanol; b) Comparison of the SERS intensity (1430 cm^{-1}) of different explosives with the same concentration of 10^{-7} M in ethanol. (I was SERS intensity of 4-ATP interacted with explosives, and I_0 was SERS intensity of 4-ATP).

groups. As shown in Figure 4, formation of the 4-ATP–TNT complex in our experiment was clearly evidenced by a new absorption peak at 529 nm and a color mutation from colorless to deep orange (the inset image of Figure 4). Depending on the Ag-S bond formation under the Ag NPs, the 4-ATP–TNT molecular bridges between nanoparticles were constructed over time. Meanwhile, the π-π conjugated structures between TNT and 4-ATP could effectively promote the electronic transfer, leading to enhanced Raman signals. The places where TNT was located may have induced the formation of "hot spots" for SERS. When the 532-nm laser was used to obtain the Raman spectrum, the complexing chromophore absorbed the light and brought about the electronic resonance of the molecular bridge and thus the enhancement of the 4-ATP Raman signals. At the same time, the spectral overlap between the chromophore absorption and the surface plasmon of the ZnO–Ag hybrid may have led to the surface resonance enhancement.

Selectivity response for nitrophenylamine explosives of modified SERS substrate

To further ascertain the recognition selectivity of the 4-ATP-modified ZnO–Ag platform, we prepared other structurally similar nitrated-explosive detection systems (10^{-7} M in ethanol)

such as picric acid (PA), 2-nitrotoluene (NT), and 2, 4-dinitrotoluene (DNT). Figure 5 showed a series of Raman spectra of 4-ATP-modified (10^{-8} M) ZnO–Ag NF hybrids with different structurally similar nitrated explosives. It was obvious that the Raman activity was not as sensitive to TNT as it was to PA, DNT, and NT at the same concentration. Compared to TNT, weaker enhancements were observed for PA, DNT, and NT. As the TNT molecule contained three electron-withdrawing nitro groups, the negative charges might be dispersed throughout the entire molecular structure, inducing a strongly reduced electron density of the aromatic ring. For NT, its single nitro group might have largely reduced the effective charge transfer between the molecules and 4-ATP. Although DNT was similar to TNT in molecular structure, it exhibited weaker SERS enhancement. The main explanation was that the negative charges could not be dispersed throughout the entire DNT molecular structure because of the lack of a nitro group, suggesting that DNT cannot likely form the effective charge-transfer complex chromophore with 4-ATP.[7b] PA had a structure that was most similar to TNT's, but it exhibited weaker SERS enhancement than TNT and stronger SERS enhancement than DNT. The reason might be that despite the presence of the three electron-withdrawing nitro groups, the strong negative ligand –OH could have easily lost a proton. Then the remaining structure $–O^-$ reduced the effective charge transfer between the molecules and 4-ATP, induced a weaker "hot spot" for strong local electric fields and exhibited a weaker SERS enhancement than TNT. Therefore, these comparisons suggested that the good SERS selectivity to TNT was due to the strong π-π conjugated structures between TNT and 4-ATP that could effectively promote the electronic transfer. Besides, the large SERS enhancement based on the 4-ATP-modified ZnO–Ag NF hybrids could be mainly manipulated by the number of nitro substituent in the nitroaromatic molecules. All these experiments indicated that the 4-ATP-functionalized ZnO–Ag NF hybrids provided an effective SERS platform for TNT detection with good sensitivity and selectivity.

Conclusions

In summary, we have demonstrated a simple method to fabricate Ag NPs with ZnO hybrids as effective SERS substrates via a facile hydrothermal approach and physical sputtering. The resultant flower-like hybrid nanostructures functionalized with 4-ATP can be used as SERS substrates with excellent signal enhancement ability. These highly active substrates allow for detection of common plastic explosive materials such as 2, 4, 6-trinitrotoluene, a leading example of nitroaromatic explosives. Our results suggest that TNT concentrations as low as 5×10^{-9} M can be accurately detected using the described SERS substrates. The technique reported here offers a simple and sensitive approach to the detection of TNT that exhibited better selectivity for TNT than other explosives with similar structures. The possibility of building a robust Raman-based assay platform was demonstrated. Further studies on the exploitation of other substrates for SERS applications are underway.

Acknowledgements

We thank Professor Jianhua Wang for kind help and beneficial discussions.

This work was supported by the National Natural Science Foundation (Nos. 21302176); Cultivate Young Talents Foundation of CAEP (Nos. QNRC-201206); the Development Foundation of CAEP (No. 2013B0302042).

Notes and references

[a] *Institute of Chemical Materials, China Academy of Engineering Physics, Mianyang 621900, China;*
[b] *Key Laboratory of Materials Physics, Anhui, Key Laboratory of Nanomaterials and Nanostructures, Institute of Solid State Physics, Chinese Academy of Sciences, Hefei, 230031, China.*
**Address for correspondence. Email: xuan.hellen@gmail.com*

† Electronic Supplementary Information (ESI) available: [details of any supplementary information available should be included here]. See DOI: 10.1039/b000000x/

1 (a) K. K. Kartha, S. S. Babu, S. Srinivasan, A. Ajayaghosh, *J. Am. Chem. Soc.*, 2012, **134**, 4834-4841; (b) R. S. Golightly, W. E. Doering, M. Natan, *Acs. Nano.*, 2009, **3**, 2859-2869.
2. (a) L. Senesac, T. Thundat, *Mater. Today* ,2008, **3**, 28-36; (b) K. Kneipp, H. Kneipp, *Accounts. Chem. Res.* , 2006, **39**, 443-450.
3. (a) W. Chen, N. B. Zuckerman, J. P. Konopelski, S. W. Chen, *Anal. Chem.* 2010, **82**, 461-465; (b) D. T. McQuade, A. E. Pullen, T. M. Swager, *Chem. Rev.* 2000, **100**, 2537-2574; (c) T. Naddo, Y. K. Che, W. Zhang, K. Balakrishnan, X. M. Yang, M. Yen, J. C. Zhao, J. S. Moore, L. Zang, *J. Am. Chem. Soc.*, 2007, **129**, 6978-6979; (d) S. J. Toal, D. Magde, W. C. Trogler, *Chem. Commun.*, 2005, **43**, 5465-5467; (e) H. Sohn, M. J. Sailor, D. Magde, W. C. Trogler, *J. Am. Chem. Soc.*, 2003, **125**, 3821-3830.
4. (a) J. S. Yang, T. M. Swager, *J. Am. Chem. Soc.*, 1998, **120**, 5321-5322; (b) S. J. Toal, W. C. Trogler, *J. Mater. Chem.*, 2006, **16**, 2871-2883.
5. D. Gao, Z. Wang, B. Liu, L. Ni, M. Wu, Z. Zhang, *Anal. Chem.*, 2008. **80**, 8545-8553.
6. (a) M. Cerruti, J. Jaworski, D. Raorane, C. Zueger, J. Varadarajan, C. Carraro, S. W. Lee, R. Maboudian, A. Majumdar, *Anal. Chem,* 2009, **81**, 4192-4199; (b) M. Riskin, R. T. Vered, T. Bourenko, E. Granot, I. Willner, *J. Am. Chem. Soc.*, 2005, **127**, 6744-6751.
7. (a)Y. Jiang, H. Zhao, N. Zhu, Y. Lin, P. Yu, L. Mao, *Angew. Chem. Int. Ed.* 2008, **47**, 8601-8604; (b) S. S. R. Dasary, H. Yu, P. C. Ray, *J. Am. Chem. Soc.*, 2009, **131**, 13806-13812; (c) X. G. Meng, *Langmuir*, 2011, **27**, 13773-13779.
8. (a) K. A. Willets, R. P. Van Duyne, *Annu. Rev. Phys. Chem.*, 2007, **58**, 267-297; (b) J. Kneipp, H. Kneipp, K. Kneipp, *Chem. Soc. Rev.*, 2008, **37**, 1052-1060; (c) Yufeng Fang, Xinlu Cheng, Chaoyang Zhang, Yang Zhou, *Chinese Journal of Energetic Materials*, 2014, **22**, 116-123.
9. M. López-López, C. García-Ruiz, *Trends in Analytical Chemistry*, 2014, **54**, 36-44.
10. (a) X. Zhou, H. L. Liu, L. B. Yang, J. H. Liu, *Analyst*, 2013, **138**, 1858-1864 ; (b) P. R. Sajanlal, T. Pradeep, *Nanoscale*, 2012, **4**, 3427-3437; (c) A. Chou, E. Jaatinen, R. Buividas, G. Seniutinas, S. Juodkazis, E. L. Izake, P. M. Fredericks, *Nanoscale*, 2012, **4**, 7419-7424; (d) T. Yu, J. Zeng, B. Lim, Y. N. Xia, *Adv. Mater.*, 2010, **22**, 5188-5192; (e) S. J. Jeong, H. S. Moon, J. U. Kim, S. O. Kim, *Nano Lett.*, 2010, **10**, 3500-3505.
11. (a) J. G. Fan, Y. P. Zhao, *Langmuir,* 2008, **24**, 14172-14175; (b) S. M. Morton, L. J. Jensen, *J. Am. Chem. Soc.*, 2009, **131**, 4090-4098; (c) C. Cheng, B. Yan, Z. Shen, H. Yu, H. J. Fan, *ACS Appl. Mater. Interfaces*, 2010, **2**, 1824-1828; (d) M. L. Zhang, X. Fan, H. W. Zhou, N. B. Wong, S. T. Lee, *J. Phys. Chem. C*, 2010, **114**, 1969-1975.
12. (a) H. B. Tang, G. W. Meng, Q. Huang, Z. Zhang, Z. L. Huang, *Adv. Funct. Mater.*, 2012, **22**, 218-224; (b) P. Xu, N. H. Mack, S. H. Jeon, S. K. Doorn, X. Han, H. L. Wang, *Langmuir*, 2010, **26**, 8882-8886; (c) S. Xiong, B. Xi, C. Wang, D. Xu, X. Feng, Z. Zhu, Y. Qian, *Adv.*

Funct. Mater., 2007, **17**, 2728-2738; (d) Y. Shao, J. Sun, L. Gao, *J. Phys. Chem. C*, 2009, **113**, 6566-6572.

13. (a) M. M. Liu, W. Chen, *Biosensors and Bioelectronics*, 2013, **46**, 68-73; (**b**) K. A. Mahmoud, M. Zourob, *Analyst*, 2013, **138**, 2712-2719; (c) L. B. Yang, L. A. Ma, G. Y. Chen, J. H. Liu, Z. Q. Tian, *Chem. Eur. J.* , 2010, **16**, 12683-12693; (d)M. Riskin, R. Tel-Vered, O. Lioubashevski, I. Willner, *J. Am. Chem. Soc.*, 2008, **130**, 9726-9733; (e) H. B. Zhou, Z. P. Zhang, C. L. Jiang, G. J. Guan, K. Zhang, Q. S. Mei, R. Y. Liu, S. H. Wang, *Anal. Chem.*, 2011, **83**, 6913-6917.
14. (a) K. L. Meagley, S. P. Garcia, *Cryst. Growth Des.*, 2012, **12**, 707-713; (b) D. B. Zhang, S. J. Wang, K. Cheng, S. X. Dai, B. B. Hu, X. Han, Q. Shi, Z. L. Du, *ACS Appl. Mater. Interfaces*, 2012, **4**, 2969-2977.
15. C. Ruan, G. Eres, W. Wang, Z. Zhang, B. Gu, *Langmuir*, 2007, **23**, 5757-5759.
16. (a) L. H. Lu, I. Randjelovic, R. Capek, N. Gaponik, *A.* Eychmüller *Chem. Mater.*, 2005, **17**, 5731-5736; (b) H. L. Liu, Y. Sun, Z. Jin, L. B. Yang, J. H. Liu, *Chem. Sci.*, 2013, **4**, 3490-3496; (c) H. L. Liu, L. B. Yang, H. W. Ma, Z. M. Qi, J. H. Liu, *Chem. Commun.*, 2011, **47**, 9360-9362; (d)H. L. Liu, D. Y. Lin, Y. D. Sun, L. B. Yang, J. H. Liu, *Chem. Eur. J.*, 2013, **19**, 8789-8796.
17. (a) A. C. SantAna, T. C. R. Rocha, P. S. Santos, D. Zanchet, M. L. A. Temperini, *J. Raman Spectrosc.* 2009, **40**, 183-190 ; (b) Y. R. Fang, Y. Z. Li, H. X. Xu, M. T. Sun, *Langmuir*, 2010, **26**, 7737-7746.
18. (a) Witlicki, E. H.; Andersen, S. S.; Hansen, S. W.; Jeppesen, J. O.; Wong, E. W.; Jensen, L.; Flood, A. H. *J. Am. Chem. Soc.* 2010, **132**, 6099-6107; (b) Hirakawa, A. Y.; Tsuboi, M. *Science* 1975, **188**, 359-361.
19. (a) C. G. Xie, Z. P. Zhang, D. P. Wang, G. J. Guan, D. M. Gao, J. H. Liu, *Anal. Chem.* 2006, **78**, 8339-8346; (b) D. M. Gao, Z. P. Zhang, M. H. Wu, C. G. Xie, G. J. Guan, D. P. Wang, *J. Am. Chem. Soc.* 2007, **129**, 7859-7866.